

Forgetting Is Regulated via Musashi-Mediated Translational Control of the Arp2/3 Complex

Nils Hadziselimovic,^{1,2,3} Vanja Vukojevic,^{1,2,3} Fabian Peter,^{1,2,3} Annette Milnik,^{1,2} Matthias Fastenrath,⁴ Bank Gabor Fenyves,⁵ Petra Hieber,^{1,2,3} Philippe Demougin,^{1,2,3} Christian Vogler,^{1,6} Dominique J.-F. de Quervain,^{1,4,6} Andreas Papassotiropoulos,^{1,2,3,6} and Attila Stetak^{1,2,3,6,*}

¹Transfaculty Research Platform Molecular and Cognitive Neurosciences, University of Basel, Birmannsgasse 8, 4055 Basel, Switzerland

²Division of Molecular Neuroscience, Department of Psychology, University of Basel, Birmannsgasse 8, 4055 Basel, Switzerland

³Biozentrum, Life Sciences Training Facility, University of Basel, Klingelbergstrasse 50/70, 4056 Basel, Switzerland

⁴Division of Cognitive Neuroscience, Department of Psychology, University of Basel, Birmannsgasse 8, 4055 Basel, Switzerland

⁵Department of Medical Chemistry, Semmelweis University, Tüzoltó u. 37-47, 1094 Budapest, Hungary

⁶University Psychiatric Clinics, University of Basel, Wilhelm Klein-Strasse 27, 4055 Basel, Switzerland

*Correspondence: a.stetak@unibas.ch

<http://dx.doi.org/10.1016/j.cell.2014.01.054>

SUMMARY

A plastic nervous system requires the ability not only to acquire and store but also to forget. Here, we report that *musashi* (*msi-1*) is necessary for time-dependent memory loss in *C. elegans*. Tissue-specific rescue demonstrates that MSI-1 function is necessary in the AVA interneuron. Using RNA-binding protein immunoprecipitation (IP), we found that MSI-1 binds to mRNAs of three subunits of the Arp2/3 actin branching regulator complex in vivo and downregulates ARX-1, ARX-2, and ARX-3 translation upon associative learning. The role of *msi-1* in forgetting is also reflected by the persistence of learning-induced GLR-1 synaptic size increase in *msi-1* mutants. We demonstrate that memory length is regulated cooperatively through the activation of *adducin* (*add-1*) and by the inhibitory effect of *msi-1*. Thus, a GLR-1/MSI-1/Arp2/3 pathway induces forgetting and represents a novel mechanism of memory decay by linking translational control to the structure of the actin cytoskeleton in neurons.

INTRODUCTION

Animals receive and respond to environmental challenges throughout their life. This vast amount of information is retained in the nervous system and ensures the behavioral plasticity of the organism. In order to maintain a highly flexible nervous system, not only the generation of memories but also forgetting (memory loss) is essential to adapt to a constantly changing environment (McGaugh, 2000).

Molecular mechanisms that underlie learning and memory formation are extensively studied, and our current knowledge provides a complex picture on the regulation of synaptic plasticity.

The activity-dependent Ca²⁺ influx during long-term potentiation (LTP), for example, activates a multitude of signaling pathways, trafficking and rearrangements of scaffold proteins (Kessels et al., 2009), protein degradation and synthesis, gene expression changes (Carlezon et al., 2005), and subsequent structural modifications of the actin cytoskeleton (Wang et al., 2006). Modulation of the actin dynamics during learning and memory mediates morphological changes of synaptic areas and is also necessary for the formation of new synaptic connections in vertebrates (Bosch and Hayashi, 2012). However, until now, the molecular mechanisms that link LTP- or long-term depression-regulated signaling cascades to the structural changes of the actin cytoskeleton during learning and memory are poorly investigated.

The two classical psychological concepts of forgetting, decay and interference, are usually thought of as two distinct processes (Jonides et al., 2008; Wixted, 2004). The decay model suggests that memory passively disappears over time, whereas the interference model claims that forgetting results from competition with other memory traces (Jonides et al., 2008; Wixted, 2004). Recent studies demonstrated that active regulation of forgetting likely takes place (Berry et al., 2012; Inoue et al., 2013; Shuai et al., 2010) and that retention and loss of memory does not depend solely upon the activity of kinases and phosphatases. Active regulators of forgetting also include the small guanosine-triphosphate-binding protein Rac in *Drosophila* (Shuai et al., 2010) and a TIR-1/JNK-1 pathway in the sensory neurons in *C. elegans* (Inoue et al., 2013). These findings suggest that multiple different signaling cascades are regulating the retention and loss of memories.

RNA-binding proteins (RBPs) have recently emerged as essential modulators of mRNA distribution, translation, and degradation during proper synaptic function (Holt and Bullock, 2009). In vertebrates, *musashi1* (*msi1*) and *musashi2* (*msi2*) are two closely related members of the *musashi* (*msi*) gene family, which belongs to the RNA-recognition motif (RRM) containing proteins that interact with single-stranded RNAs (Sakakibara et al., 2002). Both MSIs are expressed in the developing and

adult nervous system. In mammals, MSI1 is mainly expressed in stem and progenitor cells and its expression decreases during differentiation (Sakakibara et al., 2001), whereas MSI2 is present also in differentiated neurons of the adult brain (Sakakibara et al., 2001). In nematodes, the sole *musashi* (*msi-1*) is widely expressed during embryogenesis and remains present in differentiated mature neurons of the adult nervous system similar to *musashi* in *Drosophila* (Hirota et al., 1999; Yoda et al., 2000). In *C. elegans*, loss of the *msi-1* gene causes a defect in male mating behavior (Yoda et al., 2000), suggesting that MSI may regulate the activity of differentiated neurons.

MSIs bind to the (G/A)_nAGU (n = 1–3) motif located in the 3' UTR of the target mRNA. Although MSI binding to this RNA sequence in vitro is well documented (Ohshima et al., 2012), so far only few in vivo targets were identified, such as *m-numb* (Imai et al., 2001), CDKN1A (Battelli et al., 2006), doublecortin (Horisawa et al., 2009), and *c-mos* in *Xenopus leavis* (Charlesworth et al., 2006). Beside these, an immunoprecipitation of RNA-binding protein coupled to microarray (RIP-ChIP) approach recently identified 64 mRNAs that were interacting with MSI in transfected human embryonic kidney 293 cells (de Sousa Abreu et al., 2009). These MSI-binding partners are mainly genes involved in proliferation, apoptosis, cell differentiation, and post-translational modification and, interestingly, include a component of the Arp2/3 actin branching regulator protein complex (*ACTR2*). Thus, its expression pattern in the nervous system and its interaction with the *ACTR2/ax-2* mRNA make *Musashi* a likely candidate that may regulate memory.

Here, we show that the *C. elegans* neuronal *musashi* gene ortholog *msi-1* regulates forgetting. Although MSI-1 is expressed in several neurons, memory length depends on the action of MSI-1 only in the AVA interneuron. We demonstrate that MSI-1 binds in vivo to the mRNA of three members of the actin branching ARP2/3 complex and regulates their protein levels via a 3' UTR-dependent translational repression. The inhibitory function of *msi-1* is also reflected in persistence of GLR-1-positive synapse size increase induced by associative learning in *msi-1(lf)* mutants. Finally, GLR-1 signaling possibly regulates both actin capping through the activity of *adducin* (*add-1*) and inhibition of actin branching mediated by *msi-1*, and these two parallel mechanisms act in concert to establish the proper memory trace. Our results suggest that MSI-1 regulates forgetting and point to a novel aspect of memory regulation linking translational repression to regulation of the actin cytoskeleton structure.

RESULTS

MSI-1 Function Accelerates Memory Loss

In an effort to identify potential genes regulating actin cytoskeleton remodeling during associative learning and memory, we performed a candidate-gene-based test using learning and memory assays in *C. elegans* (Kauffman et al., 2010; Nuttley et al., 2002; Vukojevic et al., 2012). MSI-1 represented a likely candidate based on its expression pattern and interaction with the *ACTR2/ax-2* mRNA. Thus, we investigated the potential role of a loss-of-function deletion allele *msi-1(os1)* of the sole *C. elegans* *Musashi* ortholog (Yoda et al., 2000). Because olfactory conditioning relies on normal detection of volatile attrac-

tants, we first tested the chemotaxis of *msi-1(lf)* animals toward different odorants. The chemotaxis of *msi-1(lf)* mutants to three different volatile attractants and a repellent was comparable to the response of the wild-type strain (Figure S1A available online). Furthermore, both wild-type and *msi-1(lf)* mutants showed normal locomotor behavior and responded similarly to food, indicating that *msi-1(lf)* mutants have no obvious sensory or motor defects (Figure S1B). In the negative olfactory learning assay, unconditioned wild-type and *msi-1(lf)* animals both exhibited strong chemotaxis toward diacetyl (DA) (Figure S1C). Furthermore, after a 1 hr starvation period in the presence of DA (conditioning), both wild-type and *msi-1* mutant animals displayed a strongly reduced attraction to DA, whereas starvation or DA alone (in presence of abundant food) had only a mild effect (Figure S1C). *msi-1(lf)* mutants showed normal associative learning toward DA when compared to wild-type (Figure S1C). Finally, we tested the role of *msi-1* in the ability of the animals to retain a conditioned behavior over time (short-term associative memory [STAM] and long-term associative memory [LTAM]). In STAM, animals were subjected to conditioning and tested every 10 min over a period of 1 hr for their DA preference (Figure 1A). In wild-type animals, the negative association of DA with starvation persisted during the recovery period tested (Figure 1A). *msi-1(lf)* worms showed a strong increase in memory retention (Figure 1A). Reintroduction of a wild-type 16 kb genomic fragment of the *msi-1* gene into the mutant worms fully rescued the memory phenotype (Figure 1B). Finally, we observed a similar effect of *msi-1* on memory in a salt gustatory associative learning assay (Wicks et al., 2000) (Figure S1D). The effect observed was not due to developmental defects, because RNAi silencing of *msi-1* following neuronal differentiation phenocopied the *msi-1(lf)* phenotype (Figure 1C). To further confirm a sensory-input-independent role of *msi-1*, we tested animals for their short-term positive associative memory, as described previously (Kauffman et al., 2010). In this assay, a simultaneous exposure to 2-butanone and food as a reward dramatically increased chemotaxis toward the attractant in both wild-type and *msi-1(lf)* worms to a similar extent (Figure 1D). However, the 1 hr recovery phase resulted in a recovery to almost naive behavior in wild-type animals, whereas *msi-1(lf)* mutants still exhibited strong attraction toward 2-butanone (Figure 1D). Thus, deletion of *msi-1* inhibits memory loss independently of the sensory input. Finally, we tested the effect of *msi-1* on aversive LTAM as described previously (Vukojevic et al., 2012). Although learning (aversion to DA immediately following the conditioning phase) was effective in all genotypes, we observed significant differences in LTAM retention in *msi-1(lf)* mutants compared to the wild-type worms after a 24 hr or 32 hr delay period (Figure 1E). Altogether, these results demonstrate that the *C. elegans* ortholog of *Musashi* induces a sensory-input-independent memory loss both in STAM and LTAM.

MSI-1 Function Is Necessary in the AVA Interneuron

Previously, *msi-1* expression in GABAergic neurons of the adult *C. elegans* nervous system was demonstrated (Yoda et al., 2000). In order to study in more detail the expression of MSI-1 in adult worms, we generated an *msi-1* minigene construct by fusing the 7.7 kb promoter region with *msi-1* cDNA, tag red

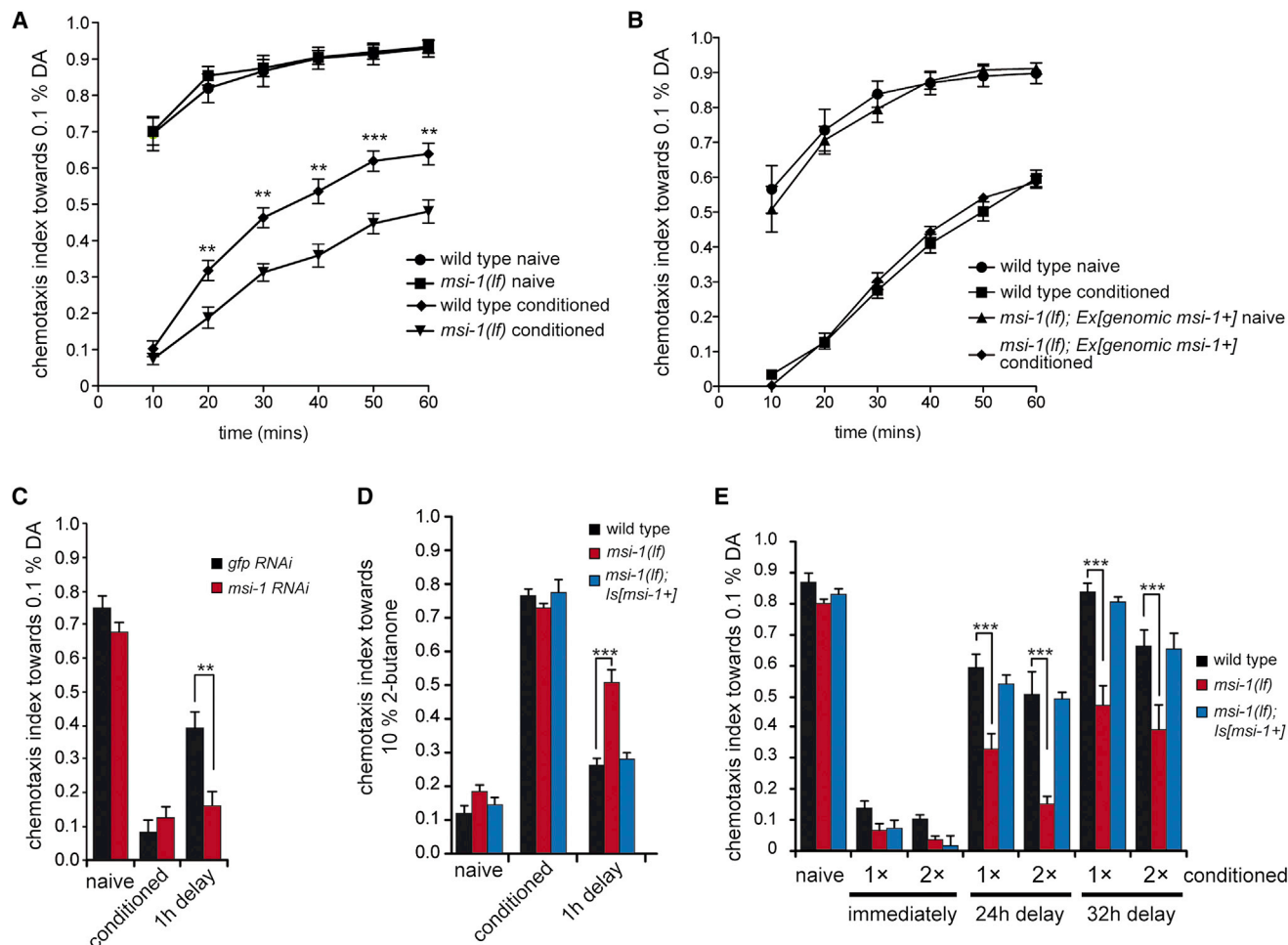


Figure 1. Loss of *C. elegans* MSI-1 Interferes with Memory Loss

(A) The STAM was tested in worms without (naive) or with conditioning, and DA preference was recorded every 10 min for 1 hr.

(B) STAM was tested in wild-type and *msi-1(lf)* mutant worms rescued with the genomic *msi-1* locus. Graph shows the sum of three independent lines.

(C) STAM conditioning of RNAi-hypersensitive worms (*nre-1 lin15b*) treated with *msi-1* or *gfp* RNAi from early L3 until adulthood. Worms were assayed toward DA without (naive) or with (conditioned) preincubation with DA or after 1 hr (1h delay).

(D) Positive STAM in different genotypes was tested as described elsewhere (Kauffman et al., 2010) toward 2-butanone immediately (conditioned) or after a 1 hr delay.

(E) Negative LTAM in the different genotypes was tested following one (1×) or two (2×) consecutive conditioning phases and DA preference was tested immediately, after 24 hr (24h delay) or 32 hr (32h delay) recovery period.

All experiments were done in triplicates and repeated at least three times. Bars represent mean ± SEM. **p < 0.01, ***p < 0.001. See also Figure S1 and Table S1.

fluorescent protein (tRFP), and the *msi-1* 3' UTR. The expression of MSI-1::tRFP was investigated in an AMPA-type glutamate-receptor-expressing GLR-1::GFP transgenic background (Figures 2A–2F). As shown on Figure 2, MSI-1 expression partially overlapped with GLR-1 expression in the adult nervous system. Besides the GABAergic neurons (RMEL, RMER, RMEV, RMED) (Yoda et al., 2000), we identified AVA, AFD, and RMD neurons that are expressing MSI-1 (Figures 2D–2F). We previously showed that the GLR-1-expressing AVA neuron is a key regulator of olfactory associative memory in *C. elegans* (Stetak et al., 2009; Vukojevic et al., 2012). In order to define the cellular requirement for MSI-1, we performed tissue-specific rescue experiments by expressing the *msi-1* cDNA under the control of the endogenous, *nmr-1*, *lim-4*, *rig-3*, or the *unc-47* promoters in the

msi-1(lf) mutant. The activity of these promoters overlaps with certain subsets of MSI-1-expressing neurons (Figure 2G), allowing us to pinpoint the cellular focus of *msi-1*. In the STAM test, the endogenous promoter as well as the *P_{nmr-1}* and *P_{rig-3}*-driven *msi-1* cDNA rescued the memory phenotype of *msi-1(lf)* mutants (Figures 2H, 2J, and 2K), whereas no rescue was observed when using *P_{lim-4}* or *P_{unc-47}* (Figures 2I and 2L).

MSI-1 Interacts with *arx-1*, *arx-2*, and *arx-3* mRNAs of the Arp2/3 Complex

Besides the identification of the cellular focus of *msi-1*, we investigated the requirement for the interaction of *msi-1* with RNA in forgetting. We generated an RNA-binding mutant form in both RRM domains of the rescuing *msi-1* cDNA by altering all three

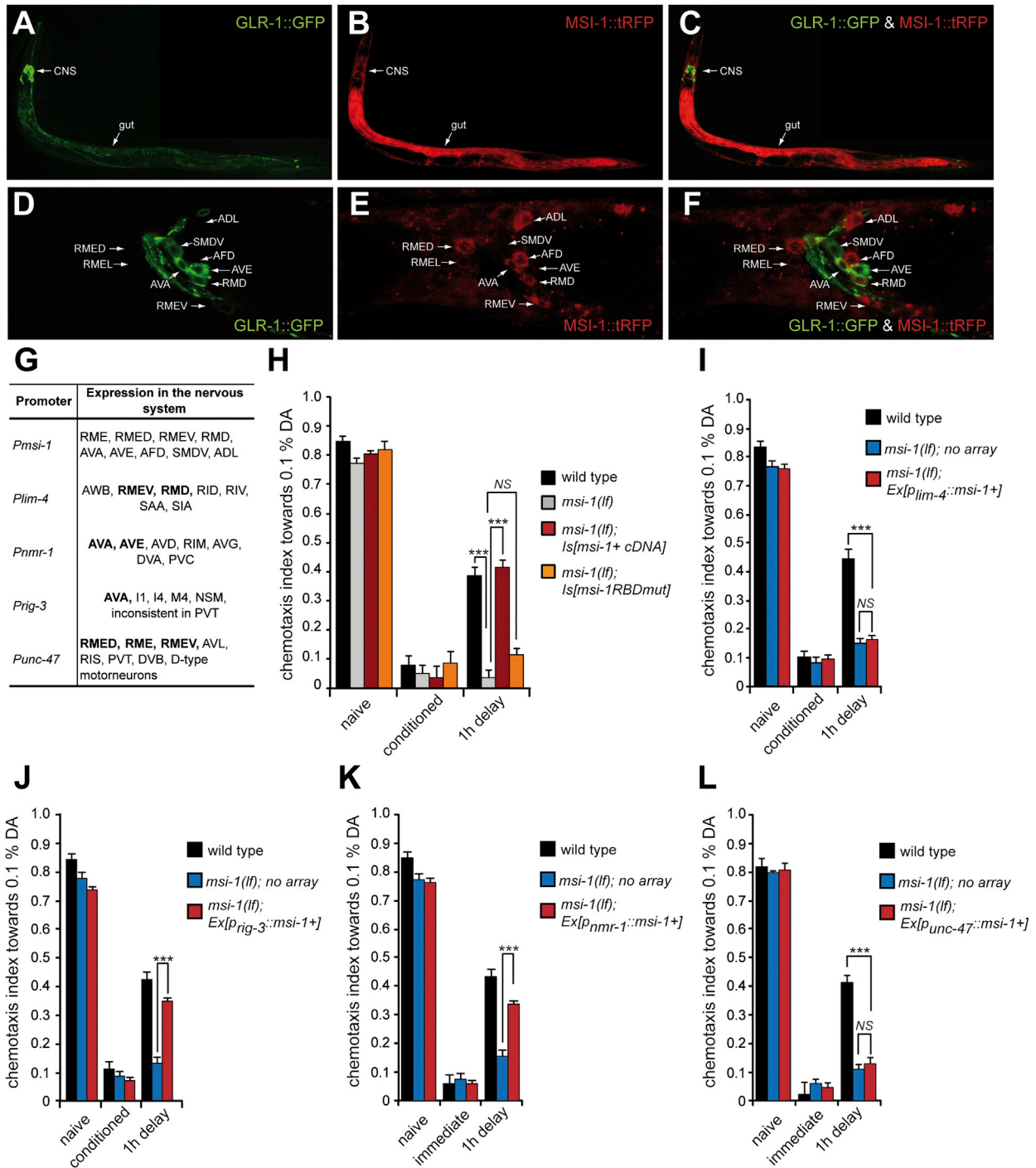


Figure 2. MSI-1 Regulates Memory Loss in the AVA Interneuron

(A–C) MSI-1 expression in the adult worm is detected in the gut and in multiple head neurons (red in A and C). MSI-1 partially overlaps with the GLR-1 expression (green in B and C). Panels shown were constructed by merging three overlapping images to reconstruct the whole animal. The black box in the top right was added using Photoshop to complete the rectangular image.

(D–F) In the head region, MSI-1 (red) was found in previously identified GABAergic neurons (RMEs) and in some GLR-1-expressing (green) cells (AVA, RMD).

(G) Expression pattern of the different neural promoters used in (H)–(L). Overlap with the *msi-1*-expressing neurons is highlighted in bold.

(H) Rescue of the forgetting defect of *msi-1(lf)* mutant worms carrying the wild-type (*msi-1+*) or an RNA-binding mutant (*RBDmut*) *msi-1* cDNA fused to Myc-tag under the control of the endogenous *msi-1* promoter.

(legend continued on next page)

conserved K to A in each domain (Figure S2) previously found to be essential for Musashi1-RNA interaction (Miyanoiri et al., 2003). In accord with the known function of MSI-1, the RNA-binding mutant *msi-1* was unable to rescue the memory phenotype of the *msi-1(lf)* mutants (Figure 2H). Thus, MSI-1 exerts its memory-related function by interacting with target RNA molecules. Among the previously identified MSI mRNA-binding partners (de Sousa Abreu et al., 2009), 14 genes are conserved in nematodes. One of these is the ACTR2/ARX-2, a member of the Arp2/3 protein complex that induces actin branching (Machesky and Gould, 1999). Because actin remodeling has a known role in synaptic plasticity (Okamoto et al., 2004), ACTR2/ARX-2 may represent a link to synapse remodeling, cortical actin structure modification, and maintenance of memory. To investigate the physical interaction between MSI-1 and the Arp2/3 protein complex, we used the integrated *msi-1(lf); ls[msi-1 minigene::myc-tag]* or as control the *msi-1(lf); ls[msi-1RBDmutant::myc-tag]* *C. elegans* strains (Figure 2H). The different MYC-tagged proteins were immunoprecipitated, the associated RNA was isolated, and the mRNA levels of the different subunits of the Arp2/3 protein complex (*arx-1* to *arx-7*) were quantified using quantitative RT-PCR (qRT-PCR). Equal amounts of bacterial reference RNAs were added to the isolated RNA before the reverse transcription and used for the quantitative PCR normalization. The relative amounts of the *arxs* RNA were compared to mock immunoprecipitations from the N2 strain (Figure 3A). We found that MSI-1 interacted with *arx-1*, *arx-2*, and *arx-3* mRNA, but not with the other four members of the Arp2/3 complex. In addition, mutation of both RNA-binding domains in MSI-1 inhibited interaction of MSI with target mRNAs (Figure 3B). Finally, we could not detect any learning-induced change in MSI-1 expression levels and alteration of the interaction between MSI-1 and its targets, suggesting that the in vivo binding of MSI-1 to the target mRNAs (*arx-1*, *arx-2*, and *arx-3*) is constitutive.

MSI-1 Regulates Translation from the *arx-1*, *arx-2*, and *arx-3* mRNAs Depending on Neuronal Activity

Next, we studied the potential regulation of the ubiquitously expressed different ARX protein levels by MSI-1. In order to monitor 3' UTR-mediated translational control in the *msi-1*-expressing set of neurons, we generated reporter constructs by fusing the promoter of *msi-1* to GFP and the 3' UTR region of the different *arx* members and established stable integrated transgenic lines. We analyzed the changes of the GFP protein levels controlled by different *arx* 3' UTRs during associative learning and short-term memory by measuring the GFP intensity of transgenic worms either in the head region or within the AVA interneuron of the treated worms. Consistent with our hypothesis, we found a strong reduction of the fluorescence signal upon STAM when GFP was under the control of the *arx-1*, *arx-2*, or *arx-3* 3' UTR (Figures 3C–3E). The 3' UTR-mediated repression was specific to associative learning, because food

withdrawal (starved) or DA alone (adapted) did not influence the GFP signal. Furthermore, the reduction in the amount of protein persisted over at least 1 hr (60 min recovery). At the same time, the GFP levels under the control of the *arx-4* or *arx-5* 3' UTR were not affected (Figures 3F and 3G). We obtained similar results when we analyzed the GFP intensities specifically in the AVA neuron (Figure S3). Finally, we tested the *gfp* mRNA levels under the control of different *arxs* 3' UTRs using qRT-PCR in order to exclude potential changes in the amount of RNA upon conditioning (Figure 3H). We found that the *gfp* mRNA levels were not affected by conditioning, further supporting the idea that the protein levels of ARX-1, ARX-2, and ARX-3 are regulated at the translational level by MSI-1.

Next, we analyzed the role of MSI-1 in the regulation of ARX-1, ARX-2, and ARX-3 protein levels by comparing GFP signals of the transgenes in wild-type or *msi-1(lf)* mutant worms. As expected, we observed a significant increase of the GFP signal in *msi-1(lf)* worms when the *gfp* was under the control of the *arx-1*, *arx-2*, or *arx-3* 3' UTR (Figures 4A–4C), whereas the levels under the regulation of the *arx-4* or *arx-5* 3' UTR were unaffected (Figures 4D and 4E). Furthermore, we could not detect a decrease of the GFP signal after conditioning when *msi-1* was deleted [*msi-1(lf)* cond]. The effect of *msi-1* deletion was rescued by the reintroduction of the wild-type copy of *msi-1* cDNA in the mutant background. Finally, the *gfp* mRNA levels were not different in the *msi-1(lf)* mutant when compared to wild-type animals (Figure 4F). Our findings show that loss of *msi-1* causes elevated protein levels and loss of downregulation of the Arp2/3 complex upon learning. Thus, translational inhibition should suppress the phenotype observed in *msi-1(lf)* worms. Indeed, cycloheximide treatment directly after conditioning fully suppressed *msi-1(lf)* memory phenotype without influencing memory in wild-type worms (Figure 4G). In contrast, cycloheximide treatment prior to conditioning interfered with memory in all genotypes, suggesting that memory acquisition and stabilization occur during the 1 hr conditioning phase independently of *msi-1* function (Figure 4H).

Increase in Arp2/3 Complex Activity in the AVA Interneuron Inhibits Memory Loss

Our results established a link between the presence of MSI-1 and the protein amount of the Arp2/3 complex. Next, we postulated that the *msi-1(lf)* memory phenotype caused by the increased amount of the Arp2/3 protein complex will be suppressed by the simultaneous reduction of the MSI-1 target RNAs. Thus, we performed RNA silencing of *arx-2* in RNAi hypersensitive strains with or without *msi-1* function and tested the memory of the treated worms. To exclude a developmental defect caused by the removal of the Arp2/3 complex, we treated nematodes with double-stranded RNA (dsRNA) after the full differentiation of the nervous system. Silencing *arx-2* in *msi-1(lf)* efficiently suppressed the mutant phenotype, whereas it had no effect in *msi-1+* worms (Figure 5A). The Arp2/3 complex

(L–L) Tissue-specific rescue of the memory loss defect of *msi-1(lf)* mutant worms carrying the *msi-1* minigene under the control of different promoters as indicated. Worms of each transgenic line were conditioned and their preference toward DA was tested immediately (conditioned) or following 1 hr recovery (1h delay). All experiments were done in triplicate and repeated in three independent experiments. Bars represent the average of three independent transgenic lines with (as indicated) or without array (no array) for each construct. Bars represent mean \pm SEM. NS, nonsignificant, *** $p < 0.001$. See also Figure S2 and Table S2.

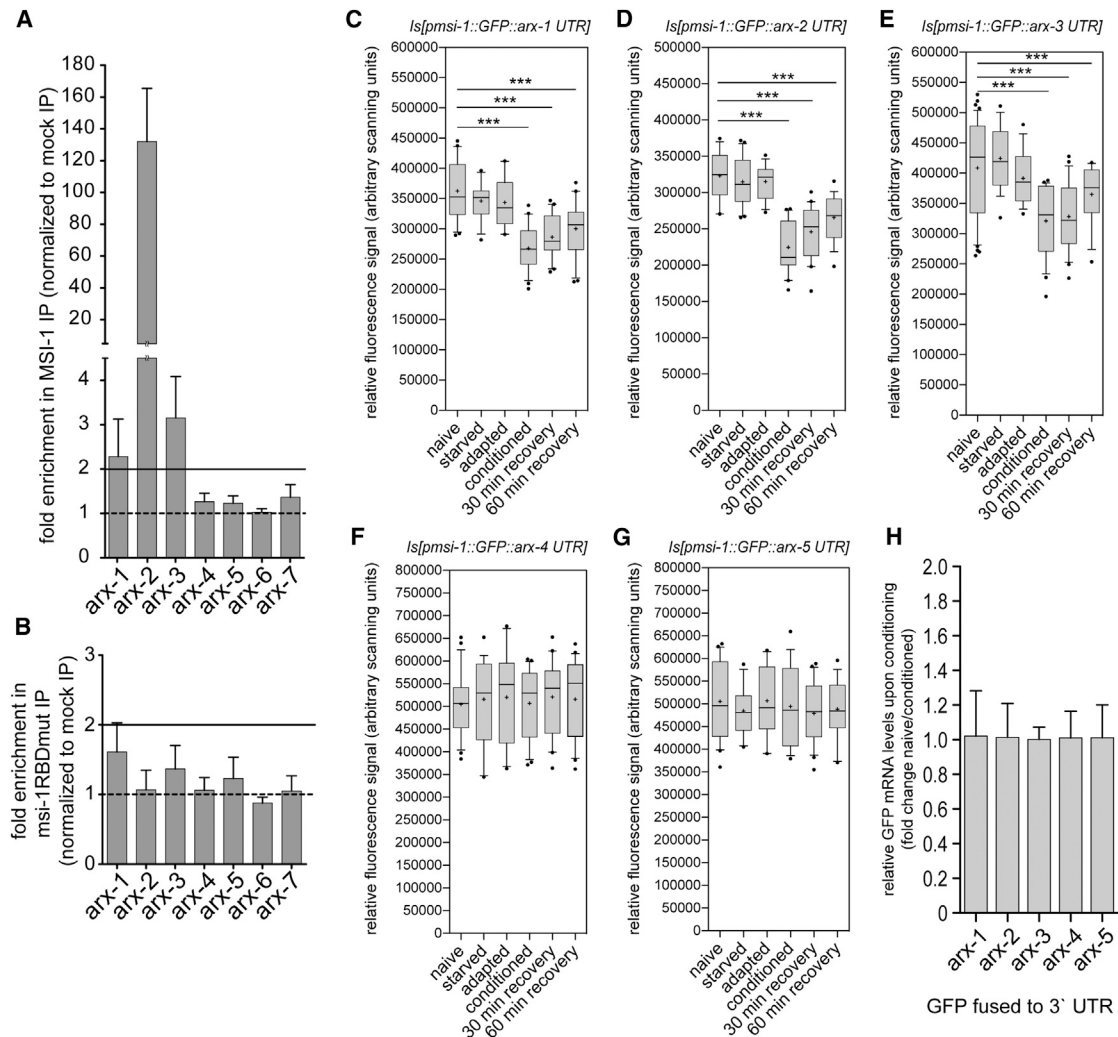


Figure 3. Translational Control of ARX-1, ARX-2, and ARX-3 during Olfactory-Associative Learning and Memory

(A) MSI-1/RNA complexes from wild-type (mock) or *msi-1(f)*; *Is[msi-1 minigene::myc-tag]* were precipitated using anti-Myc antibody, and the amounts of the different *arx* mRNAs were quantified using qRT-PCR compared to mock immunoprecipitation (IP). Dotted line represents no change; solid line shows the 2-fold enrichment threshold.

(B) The enrichment of the different *arx* mRNAs in MSI-1 IPs were measured using qRT-PCR from wild-type (mock) or *msi-1(f)*; *Is[msi-1 RDB mutant::myc-tag]* strain. Bars in (A) and (B) indicate mean \pm SEM.

(C–G) GFP intensity in integrated transgenic worms carrying 7.7 kb *msi-1* promoter, GFP, and 3' UTR of *arx-1* (C), *arx-2* (D), *arx-3* (E), *arx-4* (F), or *arx-5* (G). GFP signal was measured in untreated worms (naive), after starvation (starved), following exposure to DA alone (adapted), or immediately after DA conditioning (conditioned). GFP intensity during short-term memory was tested 30 min (30 min recovery) or 1 hr (60 min recovery) after conditioning with DA. For each condition, at least 20 animals from three independent treatments were recorded.

(H) Relative *gfp* mRNA levels were measured using qRT-PCR from total RNA isolated from naive or conditioned transgenic worms carrying different *pmsi-1::GFP::arx* 3' UTR arrays as indicated. The RNA levels were obtained in four technical replicates and three independent biological replicates.

Bars represent 10th and 90th percentile \pm whiskers in (C)–(G) and mean \pm SD in (H). *** $p < 0.001$. See also Table S3.

consists of seven subunits that interact to form the active complex (Machesky and Gould, 1999; Pollard and Beltzner, 2002). Therefore, we performed RNAi silencing of several other members of the Arp2/3 complex and found that removal of any of the subunits tested suppressed the *msi-1(f)* phenotype to a similar extent (Figure 5B). This result suggests that MSI-1 may inhibit actin cytoskeleton branching by decreasing the amount of the Arp2/3 protein complex.

The members of the N-WASP protein family, such as WSP-1, induce the activity of the Arp2/3 complex. Based on our hypothesis, a decrease in WSP-1 activity would suppress the *msi-1(f)* phenotype, whereas constitutive activation of the Arp2/3 complex would lead to increased actin branching and inhibition of memory loss, similar to loss of MSI-1 function. To decrease WSP-1 activity, we performed RNAi silencing of *wsp-1* after differentiation of the nervous system. In accord with our

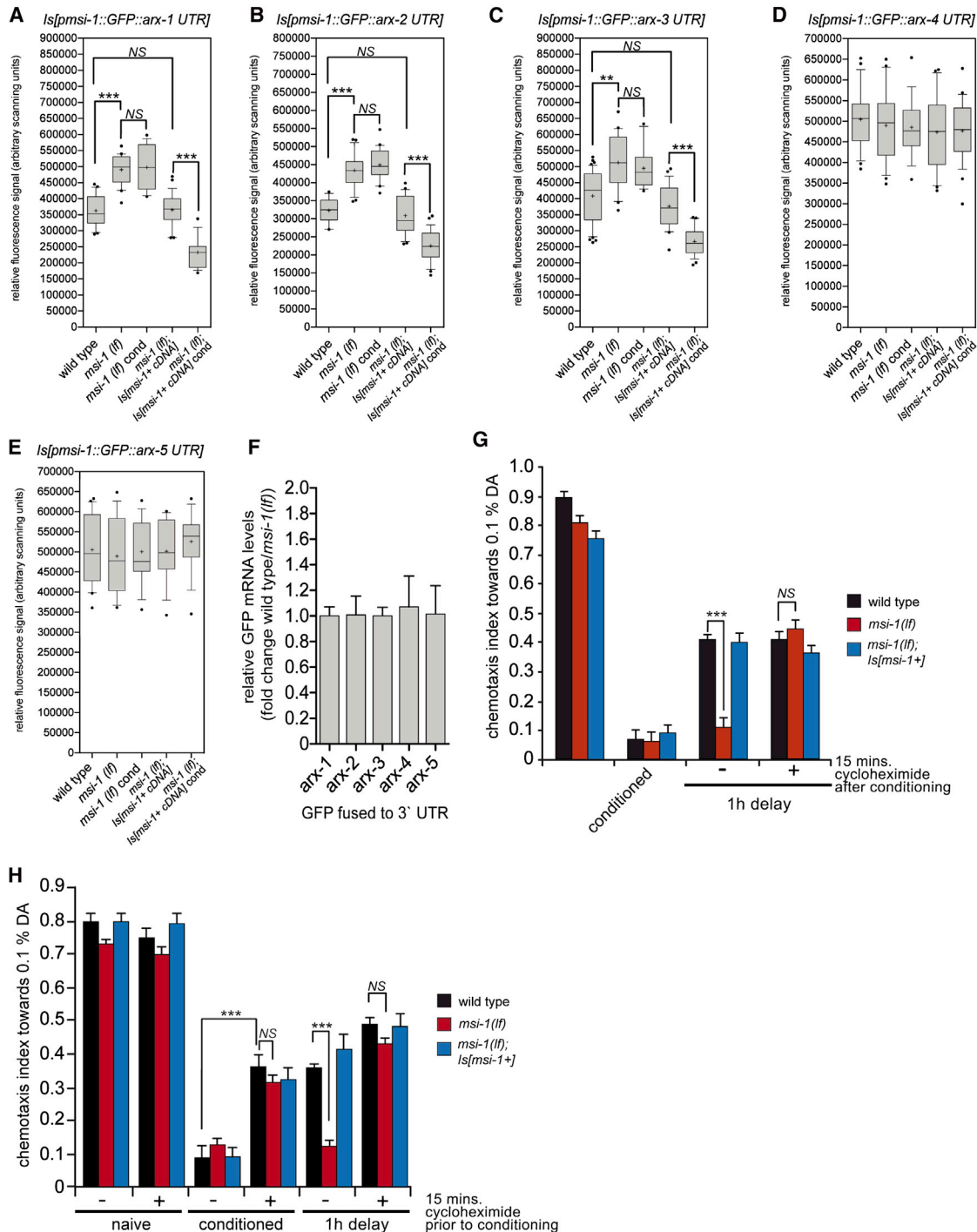
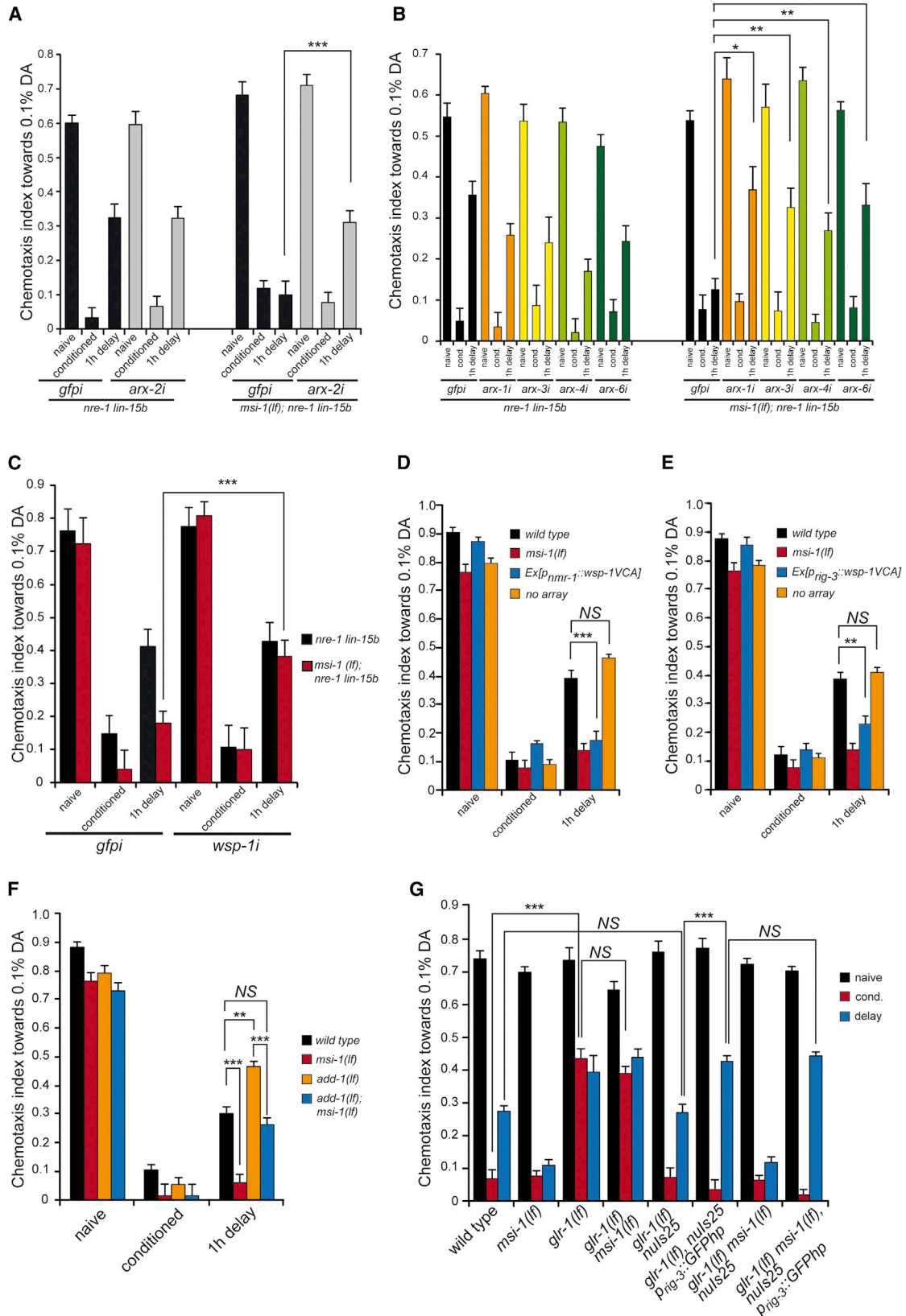


Figure 4. Translational Repression of ARX-1, ARX-2, and ARX-3 Depends on the MSI-1 Activity

(A–E) GFP intensity in integrated transgenic worms carrying 7.7 kb *msi-1* promoter, GFP and 3'UTR of *arx-1* (A), *arx-2* (B), *arx-3* (C), *arx-4* (D), or *arx-5* (E). GFP signal was measured on z-projected confocal images in untreated wild-type or *msi-1(lf)* mutants and in *msi-1(lf)* mutant worms that were conditioned with DA [*msi-1(lf)* cond]. At least 20 animals from three independent treatments were analyzed.

(F) Relative *gfp* mRNA levels were measured using qRT-PCR from total RNA isolated from wild-type or *msi-1(lf)* mutant transgenic worms carrying different *pmi-1::GFP::arx* 3' UTR arrays. The RNA levels were measured in quadruplicates for three biological samples.

(G and H) Worms with genotypes indicated were treated with 800 μ g/ml cycloheximide for 15 min (H) before or (G) immediately after conditioning, washed, and tested for chemotaxis toward DA. Bars indicate 10th and 90th percentile \pm whiskers in (A)–(E) and mean \pm SD in (F)–(H). NS, nonsignificant, ** $p < 0.01$, *** $p < 0.001$. See also Figure S3 and Table S4.



(legend on next page)

hypothesis, silencing *wsp-1* in *msi-1(lf)* efficiently suppressed the mutant phenotype (Figure 5C).

WSP-1 contains a C-terminal verprolin-, cofilin-homology, acidic region (VCA), which constitutively activates the Arp2/3 complex (Yamaguchi et al., 2000). To overactivate the Arp2/3 complex, we expressed the WSP-1 VCA fragment under the control of the *nmr-1* or *rig-3* promoters in wild-type worms. In accord with our hypothesis, expression of the WSP-1 VCA fragment under the *nmr-1* or *rig-3* promoters increased memory retention in wild-type worms similar to *msi-1* deletion (Figures 5D and 5E). This result shows that increased activity of the Arp2/3 complex in the AVA neuron is sufficient to inhibit memory loss.

Opposing Regulation Mechanisms of Actin Branching and Capping Modulate Memory Retention

In light of the role of the actin cytoskeleton in shaping synapse morphology, we next investigated the interplay between actin capping and branching in memory maintenance. We simultaneously inactivated *add-1*, an actin-capping protein that regulates memory (Vukojevic et al., 2012), and *msi-1*, which modulates the amount of the Arp2/3 complex. Although loss of *add-1* alone impaired memory (Figure 5F), the simultaneous deletion of *msi-1* suppressed this phenotype and the *msi-1(lf); add-1(lf)* double mutant showed a memory similar to wild-type animals (Figure 5F). This result shows that the two genes act in a parallel but opposing manner and that the correct balance between actin capping and branching is likely to be essential for memory regulation. We previously showed that the remodeling of actin structure through the effect of *add-1*-capping function is possibly linked to GLR-1 activity (Vukojevic et al., 2012). Here, we demonstrated that MSI-1 acts in parallel to ADD-1. We therefore tested if GLR-1 also regulates memory loss through MSI-1 by monitoring learning and memory in both *glr-1(lf) msi-1(lf)* double-mutant animals and in mutants where the *glr-1* function was deleted only in the AVA neuron [*rig-3* promoter-driven *gfp-hairpin* in *glr-1(lf)* rescued with the *glr-1::gfp* construct (*glr-1(lf), nuls25*)], in combination with removal of *msi-1*. Deletion of *glr-1* results in impaired learning that is not affected by the simultaneous deletion of *msi-1* (Figure 5G). Furthermore, AVA-specific deletion of the *glr-1* function using a previously established GFP-hairpin (Vukojevic et al., 2012) was not suppressed by the concurrent removal of *msi-1* function (Figure 5G). These results

suggest that *msi-1* acts downstream of *glr-1* in parallel to *add-1* in the AVA interneuron.

Persistence of Memory-Related Activity of AVA in *msi-1(lf)* Mutants

We measured Ca^{2+} currents upon DA stimulation at different stages of learning and memory and observed a long-lasting effect of the *msi-1(lf)* mutation on memory-related activity of AVA (Figures 6A and S4). AVA is a command interneuron characterized by high basal activity. Here, we studied AVA activity with and without DA stimulation. As shown in Figure 6A, DA reduced AVA activity in naive animals, whereas we observed a marked genotype-independent DA-induced increase in Ca^{2+} transients after conditioning. Importantly, the DA-induced elevated activity of AVA remained high in *msi-1(lf)* mutants, whereas it decreased significantly in wild-type or rescued animals after a 2 hr delay time.

Inhibition of the Arp2/3 Complex Activity Suppresses the *msi-1(lf)* Phenotype

To gain insight in the temporal requirement of *msi-1* function and to confirm that *msi-1* induces forgetting through modulation of the Arp2/3 complex, we used a selective pharmacological inhibitor (CK-666) (Nolen et al., 2009) that interferes with Arp2/3 activity and acts on actin-dependent processes in worms (Figures S4J and S4K). We applied the inhibitor to block the Arp2/3 activity at different times during STAM and LTAM. Addition of different concentrations of CK-666 prior to conditioning had no obvious effect on learning and memory acquisition but efficiently blocked the *msi-1(lf)* phenotype without influencing the wild-type behavior following a 1 hr delay (Figure 6B). We obtained similar results when the inhibitor was applied for 15 min directly after conditioning (Figure 6C), 15 or 30 min following conditioning, or even after a 23 hr delay (Figure 6D). Thus, in accord with our previous results, loss of *msi-1* function increases Arp2/3 activity, which is responsible for the observed enhanced memory in *msi-1(lf)* mutants. These results also show that *msi-1* is regulating forgetting rather than memory acquisition or consolidation.

MSI-1 Stabilizes Synaptic Size Increase upon Associative Learning

Our data suggest that *msi-1* may act on the actin cytoskeleton at the synapses of the AVA neuron. AVA projects its axon along the

Figure 5. Genetic Interaction of MSI-1 with the Arp2/3 Complex, WSP-1, and the Actin-Capping Process

(A) STAM conditioning of *arx-2* or, as a control, *gfp* RNAi-treated RNAi-hypersensitive worms with (*nre-1 lin15b*) or without *msi-1* [*msi-1(lf); nre-1 lin15b*] as indicated without (naive) or with (conditioned) preincubation with DA or after 1 hr delay following conditioning (delay).
 (B) STAM conditioning of RNAi-hypersensitive worms with (*nre-1 lin15b*) or without *msi-1* function (*msi-1; nre-1 lin15b*) treated against *gfp* or the different Arp2/3 subunits as indicated. Worms were assayed toward DA without (naive) or with (cond.) preincubation with DA in absence of food. STAM was tested after 1 hr delay following conditioning (1h delay).
 (C) STAM performance of *gfp* or *wsp-1* RNAi-treated *nre-1 lin15b* or *msi-1; nre-1 lin15b* worms as indicated were assayed toward DA prior (naive) following preincubation with DA in absence of food (conditioned) or after a 1 hr delay (1h delay).
 (D and E) STAM performance in wild-type (black), *msi-1(lf)* mutant (red), or in *msi-1(lf)* worms overexpressing constitutive active *wsp-1* VCA fragment (blue) under the control of *nmr-1* (D) or *rig-3* (E) promoter. Bars represent the average of three independent transgenic lines with (as indicated) or without array (no array).
 (F) STAM was tested in worms of genotype indicated, and DA attraction was tested prior to (naive) or following preincubation with DA in absence of food (conditioned) or after a 1 hr delay (1h delay).
 (G) STAM was tested in wild-type or mutant worms as indicated. Attraction toward DA was tested prior (naive), following preincubation with DA in absence of food (cond.) or after a 1 hr recovery (delay).
 All experiments were done in triplicate and repeated at least three times. For (D), (E), and (G), three independent transgenic lines were tested. Bars indicate mean \pm SEM. NS, nonsignificant, * $p < 0.05$, ** $p < 0.01$, *** $p < 0.001$. See also Table S5.

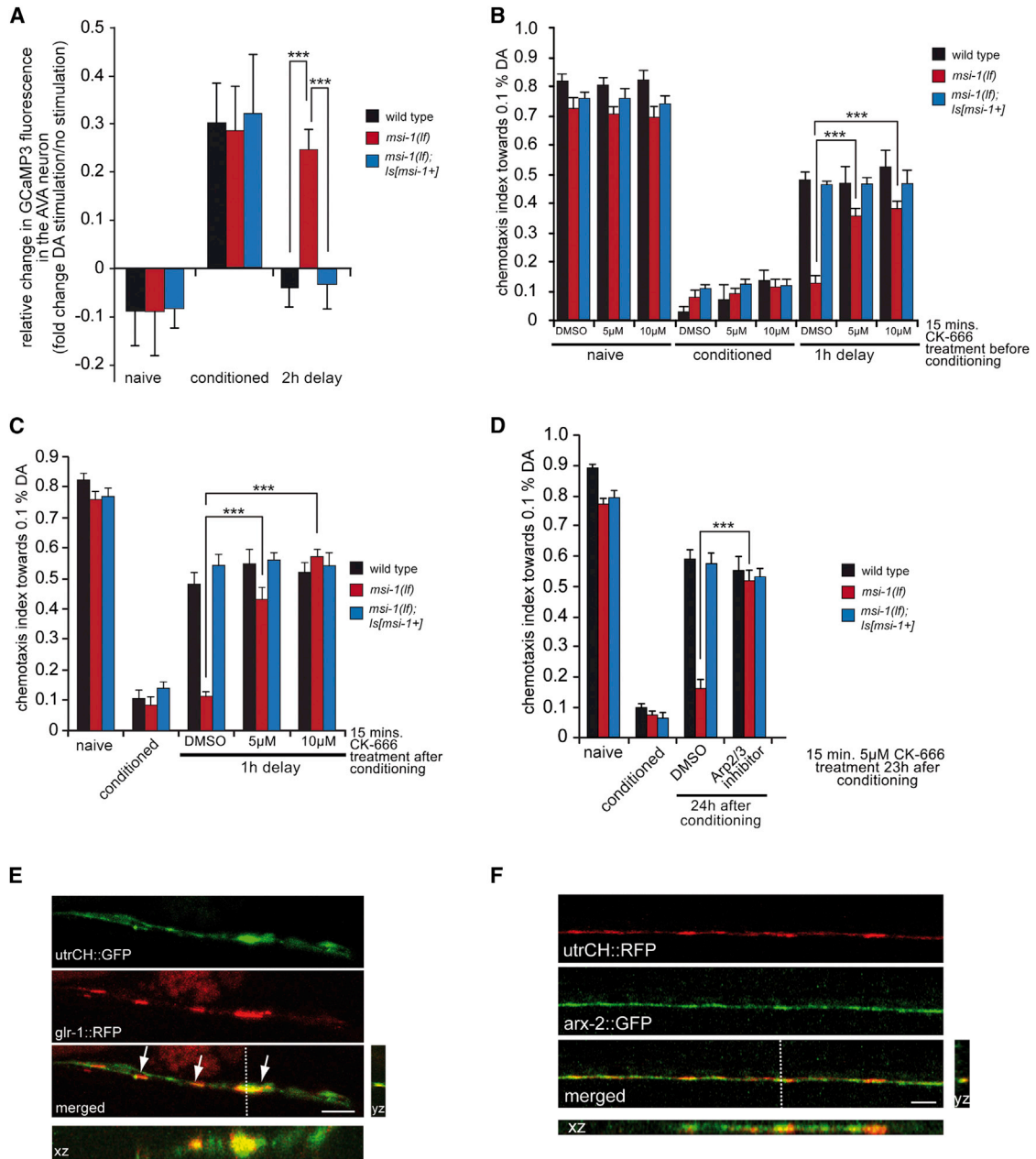


Figure 6. MSI-1 Influences Persistent Synaptic Plasticity and Acts through the Arp2/3 Complex to Regulate Forgetting

(A) Ca^{2+} was detected in transgenic animals carrying GCaMP3 under the control of the *rig-3* promoter in different genotypes as indicated. Worms were unstimulated or DA treated before (naive) or immediately after conditioning (conditioned) or after a 2 hr delay. GCaMP3 fluorescence signal was normalized to the signal of unstimulated worms ($n > 9$ for each genotype and treatment).

(B and C) Worms with indicated genotypes were treated with 5 or 10 μM CK-666 for 15 min before (B) or immediately after (C) conditioning and DA preference was tested in naive, conditioned worms, or after 1 hr delay following conditioning.

(D) Worms with indicated genotypes were treated with DMSO or 5 μM CK-666 for 15 min after 23 hr following conditioning and DA preference was tested 24 hr total delay time after conditioning as indicated. Bars represent mean \pm SEM. *** $p < 0.001$.

(E) Distribution of F-actin along the VNC was detected with utropin CH-domain fused to GFP (*utrCH::GFP*, upper panel) together with GLR-1::RFP (middle panel; arrows point to GLR-1 synapses). The position of yz-projection is marked with dotted line.

(F) Distribution of F-actin (*UtrCH::RFP*, upper panel) and ARX-2 (*ARX-2::GFP*, middle panel) along the VNC. The position of yz-projection is marked with dotted line.

Scale bar represents 1 μm . See also Figure S4 and Table S6.

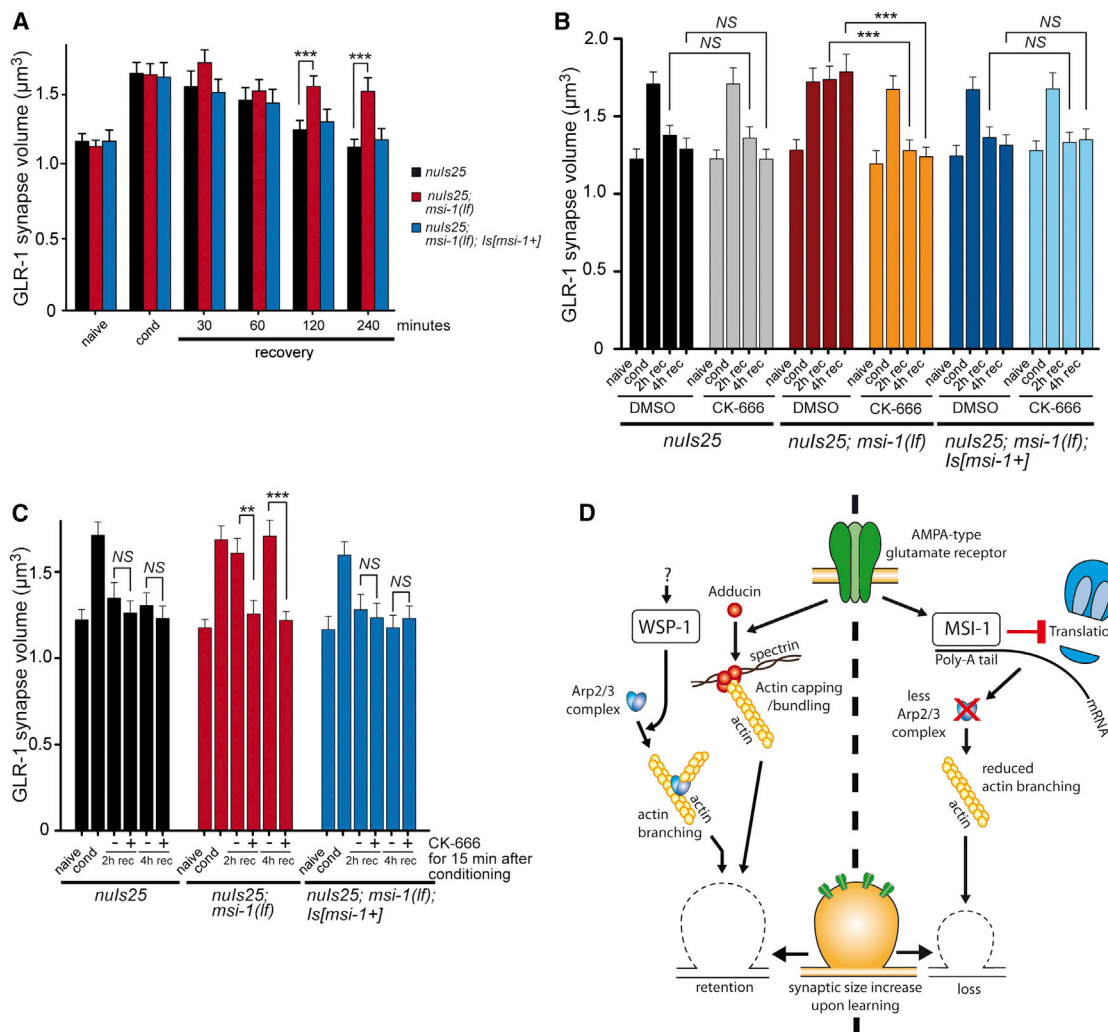


Figure 7. Deletion of MSI-1 Causes an Arp2/3-Dependent Persistent Enlargement of GLR-1-Positive Synapses Induced by Associative Learning

(A) Average volume of GLR-1::GFP synapses in the posterior VNC in wild-type and *msi-1(lf)* naive, DA-conditioned (cond) animals or following a recovery period as indicated.

(B and C) Worms with genotypes indicated were treated with 5 μM CK-666 for 15 min before (B) or immediately after (C) conditioning and synapse volumes were measured in naive, conditioned (cond), or after 2 or 4 hr delay (2h rec, 4h rec) following conditioning. At least 100 synapses were recorded for each treatment and genotype. Bars indicate mean ± SEM. NS, nonsignificant, **p < 0.01, ***p < 0.001.

(D) Model for regulation of memory loss by the MSI-1 pathway.

See also Figure S5 and Table S7.

ventral nerve chord, where it receives inputs from a large variety of neurons. Therefore, we first tested if synapses of the AVA neuron are enriched in F-actin and contain elevated levels of the Arp2/3 complex. Using confocal microscopy, we found that enriched F-actin colocalizes with GLR-1-positive synapses (Figure 6E). Furthermore, increased F-actin coincides with elevated levels of the Arp2/3 complex (Figure 6F).

Previously, we demonstrated that GLR-1-positive synapses in the *C. elegans* ventral nerve cord change their size upon associative learning (Vukojevic et al., 2012). Furthermore, persistent alteration in synaptic size correlates with memory retention. Among the GLR-1-expressing neurons projecting their axons

posterior to the vulva (AVA, AVB, AVD, and PVC), AVA receives most of the synaptic input. Laser ablation of AVA (Figure S5) deletes virtually all GLR-1 synapses representing inputs to AVA along the VNC. To measure changes in synapse morphology, we investigated GLR-1 punctae volumes posterior to the vulva in naive, DA-conditioned, and memory-consolidated wild-type and *msi-1(lf)* mutant worms. Loss of *msi-1* had no effect on GLR-1 punctae number (Figure S5G). We could not detect a difference in synapse volume between naive wild-type and mutant worms (Figure S5H). Associative learning caused a genotype-independent increase in GLR-1::GFP-positive punctae volume (Figure S5H). In contrast, GLR-1::GFP synapse

volume in wild-type animals reverted to a nearly naive level after 2 hr but remained enlarged in *msi-1(lf)* animals for the tested 4 hr period (Figure 7A). Finally, inhibition of the Arp2/3 complex with CK-666 prior to (Figure 7B) or immediately after (Figure 7C) conditioning reverted the sustained synapse enlargement observed in *msi-1(lf)* worms without influencing synapse-volume increase during learning. In summary, MSI-1 likely inhibits the persistence of the learning-induced size increase of GLR-1-positive punctae volume through the Arp2/3 complex. These results are in accord with the behavioral data and establish a link between forgetting and sustained synapse volume increase in *msi-1(lf)* mutants.

DISCUSSION

Forgetting is an essential hallmark of behavioral plasticity, although little evidence shows how memory loss is actively regulated at the molecular level (Berry et al., 2012; Inoue et al., 2013; Shuai et al., 2010). In the current study, we demonstrated that the *C. elegans musashi* (*msi-1*) is involved in forgetting independently of the sensory input or the type of memory task. Our data also imply that memory loss is actively regulated and that the learning process induces not only memory acquisition and consolidation but also forgetting. The later observation is in accord with both the proposed role of *Drosophila* Rac during memory loss (Shuai et al., 2010) and the function of the TIR-1/JNK-1 pathway in *C. elegans* (Inoue et al., 2013), suggesting that multiple molecular pathways are actively inducing the decay of memories. Although the TIR-1/JNK-1 pathway is needed in the sensory neurons (Inoue et al., 2013) to eliminate sensory memory, the data presented here propose a mechanism present in the interneurons.

Ablation of AVA, presumably the main regulator of backward movement, was previously found to abolish long reversals (Chalfie et al., 1985). Associative learning, which involves reversals and backward movement upon exposure to a chemoattractant during starvation, could lead to a sustained synaptic sensitivity of this neuron. Therefore, increase in AVA activity could be the direct mediator of avoidance behavior. This is supported by the observation that in naive animals, Ca²⁺ transients in AVA decrease upon exposure to DA whereas conditioning increases DA-dependent Ca²⁺ transients in AVA. Our results suggest that conditioning-induced activity changes in AVA likely mediate avoidance behavior. Here, we demonstrate that MSI-1 is necessary in the AVA interneuron to induce forgetting. This implies that signaling pathways in the AVA interneuron play a central role in acquisition of memories, as well as in the elimination of them, and that the balance between the two mechanisms defines the duration of memory. This hypothesis is further supported by the analysis of the *add-1*, *msi-1* double-mutant behavioral phenotype. The memory defect of the *add-1* single mutant is rescued to wild-type levels by the simultaneous deletion of *msi-1*, suggesting that the two genes act in parallel in an opposing way during regulation of memory (Figure 7D).

Among the previously identified Musashi mRNA-binding partners, ACTR2 is one of seven subunits of the Arp2/3 protein complex that serves as a nucleation core for the branching of the actin cytoskeleton (Mullins et al., 1998). Here, we found that MSI-1 interacts with the mRNAs of three subunits of the Arp2/3 complex and regulates their protein levels. Several

studies demonstrated that the function of the Arp2/3 protein complex and its proper regulation is necessary for growth of spines and establishment of synapses in vertebrates and that tight control of actin bundling and branching are required during development (Hotulainen et al., 2009). In a mature spine, the neck and the head regions contain a mixture of branched and linear actin filaments, with most of the actin bundles located in the neck and the branched actin in the head region (Korobova and Svitkina, 2010). Besides the different actin composition in synaptic spines, the cortical actin network at the synaptic membranes is also tightly regulated and modulates, for example, AMPA receptor trafficking during synaptic plasticity (Gu et al., 2010). MSI-1 likely influences, in an activity-dependent manner, the structure of the actin network at the synapse, thereby regulating the long-term persistence of size and activity increase of the synaptic areas (Figure 7D). In accordance with this, reduction of the mRNA levels of the Arp2/3 complex, or inhibition of Arp2/3 activity, suppressed the *msi-1(lf)* phenotype, suggesting that the increase of the protein levels observed in *msi-1(lf)* mutants is responsible for the inhibition of memory loss. Furthermore, overactivation of *wsp-1*, a main activator of the Arp2/3 complex (Machesky and Gould, 1999), in the AVA neuron of wild-type worms resulted in a phenotype similar to that of *msi-1* mutants. Interestingly, the activity of the Arp2/3 complex influences memory retention but has no obvious role in memory acquisition. Furthermore, CK-666 was effective 23 hr after conditioning (i.e., at a time point where memory is already consolidated), suggesting a regulation of forgetting rather than memory formation through the Arp2/3 complex. Thus, actin likely plays different roles at various stages of learning and memory. Our results suggest a novel regulation mechanism by which translational inhibition reduces the activity of the Arp2/3 complex, which may result in a less complex cortical actin network. The reduction of the actin network complexity diminishes the persistence time of enlarged synapses. This reduction may represent a structural mechanism of forgetting (Figure 7D).

The complex regulation of the actin cytoskeleton in memory is also reflected in the genetic interaction of actin capping (*add-1* mutant) and actin branching (*msi-1* deletion). Increased capping activity is necessary to stabilize synapses, and an AMPA-type glutamate receptor (GLR-1) signaling pathway in the AVA neuron likely increases actin capping through the activation of adducin (Vukojevic et al., 2012). On the other hand, intact GLR-1 function seems to be a prerequisite for the downstream MSI-1-mediated forgetting machinery (Figure 7D). Thus, activation of the GLR-1 receptor activates memory stabilization and at the same time initiates memory removal. Our results suggest that two parallel mechanisms regulate the complexity of the actin cytoskeleton and that the balance between these mechanisms is crucial for the retention of memories. It is important to stress, however, that at this stage, it is not possible to draw detailed temporal and mechanistic conclusions with regard to how MSI-1- or ADD-1-related molecular changes alter the neural networks involved at different stages of memory maintenance. The elucidation of the precise mechanisms should be a focus of further studies, because an imbalance of these mechanisms may result in altered memory function that could also play a role in memory-related disorders.

EXPERIMENTAL PROCEDURES

General Methods and Strains Used

Standard methods were used for maintaining and manipulating *C. elegans* (Brenner, 1974). The *C. elegans* Bristol strain, variety N2, was used as the wild-type reference strain in all experiments. A detailed list of the alleles and transgenes used is provided in [Extended Experimental Procedures](#). Transgenic lines were generated by injecting DNA at a concentration of 10–100 ng/μl into both arms of the syncytial gonad of worms as described previously (Mello et al., 1991). *p_{sur-5}::mDsRed* or *pRF4[rol-6D]* was used as a transformation marker at 10 ng/μl concentration. Chromosomal integration of extrachromosomal arrays was done by UV radiation for 10 s. Following integration, generated strains were four-times backcrossed to the wild-type strain. For RNAi experiments, the RNAi-hypersensitive *nre-1(hd20) lin15b(hd126)* strain was used. Early L3 stage worms were fed with bacteria containing dsRNA, and the P₀ generation was tested for behavior.

STAM and LTAM were assessed as described previously (Stetak et al., 2009). Briefly, conditioning was performed for 1 hr without food in the presence of 2 μl undiluted chemoattractant spotted on the lid of 10 cm CTX plates (5 mM KH₂PO₄/K₂HPO₄ [pH 6.0], 1 mM CaCl₂, 1 mM MgSO₄, 2% agar). Naive and conditioned worms were given a choice between a spot of 0.1% DA in ethanol with 20 mM sodium-azide and a counter spot with ethanol and sodium-azide. After a delay time, animals were counted and the chemotaxis index was calculated as described previously (Bargmann et al., 1993). A total of 50–200 animals were used in each technical and biological replicate. For the time-course experiment, naive and conditioned worms were given a choice between a spot of 0.1% DA in ethanol with 20 mM sodium-azide and a counter spot with ethanol on 6 cm plates. Animals were counted every 10 min for 1 hr and chemotaxis index was calculated as described previously (Bargmann et al., 1993). The different inhibitors were applied by soaking the worms in M9 supplemented with the inhibitor at the given concentrations.

Locomotory Rate Assays

Assays were performed on a bacterial lawn as described elsewhere (Stetak et al., 2009). Briefly, worms were grown under uncrowded conditions with or without food for 1 hr and 2 min after transfer to 6 cm plates seeded with OP₅₀, and the number of body bends was counted for 1 min for at least ten animals from each strain.

Fluorescence Microscopy

GFP (or tRFP)-tagged proteins were detected with a Zeiss Axiovert 200 M LSM 5 Pascal confocal microscope as described in [Extended Experimental Procedures](#). For synapse volume measurements, animals were immobilized and GLR-1::GFP were recorded posterior to the vulva. Quantification was performed using the ImageJ Object Counter 3D plugin. Calcium transients using GCaMP3 fluorescence calcium indicator were detected with a Zeiss Axioptan 2 fluorescent microscope and quantified with ImageJ.

RNA-Binding Protein Immunoprecipitation and Real-Time RT-PCR

Total RNA was isolated from synchronized adult worms using standard protocol. Coimmunoprecipitation was performed as previously described (Roy et al., 2002) from synchronized adult worms, and 400 ng RNA was reverse transcribed using a mix of random decamers (Ambion) and anchored oligo(dT)₂₀ primer (Invitrogen). Real-time PCR was performed using the SyBr Fast kit (Kapa Biosystems) according to manufacturer's recommendations in a Rotor Gene-6000 instrument (Corbett Research). Expression levels were normalized to *tba-1* and *cdc-42* using a geometric mean of their level of expression, and the fold change was calculated using QBasePlus software (Biogazelle).

Statistical Analysis

A detailed description of the statistical analysis can be found in [Extended Experimental Procedures](#), and [Tables S1, S2, S3, S4, S5, S6, S7, and S8](#) list statistical significance.

SUPPLEMENTAL INFORMATION

Supplemental Information includes Extended Experimental Procedures, five figures, and eight tables and can be found with this article online at <http://dx.doi.org/10.1016/j.cell.2014.01.054>.

ACKNOWLEDGMENTS

We are grateful to Anne Spang and Jean Pieters for generously sharing methods, reagents, and instruments and to Alex Hajnal for his valuable comments on the manuscript and for laser ablation tools. We also like to thank the Caenorhabditis Genetic Center (supported by the National Institutes of Health Office of Research Infrastructure Programs grant P40 OD010440) for providing nematode strains. The Forschungsfonds of the University of Basel (DPE2112 to A.S.) and the Swiss National Science Foundation (Sinergia grants CRSIK0_122691 and CRSI33_130080 to D.J.-F.d.Q. and A.P.) supported this work.

Received: July 9, 2013

Revised: November 27, 2013

Accepted: January 17, 2014

Published: March 13, 2014

REFERENCES

- Bargmann, C.I., Hartwig, E., and Horvitz, H.R. (1993). Odorant-selective genes and neurons mediate olfaction in *C. elegans*. *Cell* **74**, 515–527.
- Battelli, C., Nikopoulos, G.N., Mitchell, J.G., and Verdi, J.M. (2006). The RNA-binding protein Musashi-1 regulates neural development through the translational repression of p21WAF-1. *Mol. Cell. Neurosci.* **31**, 85–96.
- Berry, J.A., Cervantes-Sandoval, I., Nicholas, E.P., and Davis, R.L. (2012). Dopamine is required for learning and forgetting in *Drosophila*. *Neuron* **74**, 530–542.
- Bosch, M., and Hayashi, Y. (2012). Structural plasticity of dendritic spines. *Curr. Opin. Neurobiol.* **22**, 383–388.
- Brenner, S. (1974). The genetics of *Caenorhabditis elegans*. *Genetics* **77**, 71–94.
- Carlezon, W.A., Jr., Duman, R.S., and Nestler, E.J. (2005). The many faces of CREB. *Trends Neurosci.* **28**, 436–445.
- Chalfie, M., Sulston, J.E., White, J.G., Southgate, E., Thomson, J.N., and Brenner, S. (1985). The neural circuit for touch sensitivity in *Caenorhabditis elegans*. *J. Neurosci.* **5**, 956–964.
- Charlesworth, A., Wilczynska, A., Thampi, P., Cox, L.L., and MacNicol, A.M. (2006). Musashi regulates the temporal order of mRNA translation during *Xenopus* oocyte maturation. *EMBO J.* **25**, 2792–2801.
- de Sousa Abreu, R., Sanchez-Diaz, P.C., Vogel, C., Burns, S.C., Ko, D., Burton, T.L., Vo, D.T., Chennasamudaram, S., Le, S.Y., Shapiro, B.A., and Penalva, L.O. (2009). Genomic analyses of musashi1 downstream targets show a strong association with cancer-related processes. *J. Biol. Chem.* **284**, 12125–12135.
- Gu, J., Lee, C.W., Fan, Y., Komlos, D., Tang, X., Sun, C., Yu, K., Hartzell, H.C., Chen, G., Bamberg, J.R., and Zheng, J.Q. (2010). ADF/cofilin-mediated actin dynamics regulate AMPA receptor trafficking during synaptic plasticity. *Nat. Neurosci.* **13**, 1208–1215.
- Hirota, Y., Okabe, M., Imai, T., Kurusu, M., Yamamoto, A., Miyao, S., Nakamura, M., Sawamoto, K., and Okano, H. (1999). Musashi and seven in absentia downregulate Tramtrack through distinct mechanisms in *Drosophila* eye development. *Mech. Dev.* **87**, 93–101.
- Holt, C.E., and Bullock, S.L. (2009). Subcellular mRNA localization in animal cells and why it matters. *Science* **326**, 1212–1216.
- Horisawa, K., Imai, T., Okano, H., and Yanagawa, H. (2009). 3'-Untranslated region of doublecortin mRNA is a binding target of the Musashi1 RNA-binding protein. *FEBS Lett.* **583**, 2429–2434.

- Hotulainen, P., Llano, O., Smirnov, S., Tanhuanpää, K., Faix, J., Rivera, C., and Lappalainen, P. (2009). Defining mechanisms of actin polymerization and depolymerization during dendritic spine morphogenesis. *J. Cell Biol.* *185*, 323–339.
- Imai, T., Tokunaga, A., Yoshida, T., Hashimoto, M., Mikoshiba, K., Weinmaster, G., Nakafuku, M., and Okano, H. (2001). The neural RNA-binding protein Musashi1 translationally regulates mammalian numb gene expression by interacting with its mRNA. *Mol. Cell. Biol.* *21*, 3888–3900.
- Inoue, A., Sawatari, E., Hisamoto, N., Kitazono, T., Teramoto, T., Fujiwara, M., Matsumoto, K., and Ishihara, T. (2013). Forgetting in *C. elegans* is accelerated by neuronal communication via the TIR-1/JNK-1 pathway. *Cell Rep.* *3*, 808–819.
- Jonides, J., Lewis, R.L., Nee, D.E., Lustig, C.A., Berman, M.G., and Moore, K.S. (2008). The mind and brain of short-term memory. *Annu. Rev. Psychol.* *59*, 193–224.
- Kauffman, A.L., Ashraf, J.M., Corces-Zimmerman, M.R., Landis, J.N., and Murphy, C.T. (2010). Insulin signaling and dietary restriction differentially influence the decline of learning and memory with age. *PLoS Biol.* *8*, e1000372.
- Kessels, H.W., Kopec, C.D., Klein, M.E., and Malinow, R. (2009). Roles of star-gazin and phosphorylation in the control of AMPA receptor subcellular distribution. *Nat. Neurosci.* *12*, 888–896.
- Korobova, F., and Svitkina, T. (2010). Molecular architecture of synaptic actin cytoskeleton in hippocampal neurons reveals a mechanism of dendritic spine morphogenesis. *Mol. Biol. Cell* *21*, 165–176.
- Machesky, L.M., and Gould, K.L. (1999). The Arp2/3 complex: a multifunctional actin organizer. *Curr. Opin. Cell Biol.* *11*, 117–121.
- McGaugh, J.L. (2000). Memory—a century of consolidation. *Science* *287*, 248–251.
- Mello, C.C., Kramer, J.M., Stinchcomb, D., and Ambros, V. (1991). Efficient gene transfer in *C. elegans*: extrachromosomal maintenance and integration of transforming sequences. *EMBO J.* *10*, 3959–3970.
- Miyanoiri, Y., Kobayashi, H., Imai, T., Watanabe, M., Nagata, T., Uesugi, S., Okano, H., and Katahira, M. (2003). Origin of higher affinity to RNA of the N-terminal RNA-binding domain than that of the C-terminal one of a mouse neural protein, musashi1, as revealed by comparison of their structures, modes of interaction, surface electrostatic potentials, and backbone dynamics. *J. Biol. Chem.* *278*, 41309–41315.
- Mullins, R.D., Heuser, J.A., and Pollard, T.D. (1998). The interaction of Arp2/3 complex with actin: nucleation, high affinity pointed end capping, and formation of branching networks of filaments. *Proc. Natl. Acad. Sci. USA* *95*, 6181–6186.
- Nolen, B.J., Tomasevic, N., Russell, A., Pierce, D.W., Jia, Z., McCormick, C.D., Hartman, J., Sakowicz, R., and Pollard, T.D. (2009). Characterization of two classes of small molecule inhibitors of Arp2/3 complex. *Nature* *460*, 1031–1034.
- Nuttley, W.M., Atkinson-Leadbetter, K.P., and Van Der Kooy, D. (2002). Serotonin mediates food-odor associative learning in the nematode *Caenorhabditis elegans*. *Proc. Natl. Acad. Sci. USA* *99*, 12449–12454.
- Ohyama, T., Nagata, T., Tsuda, K., Kobayashi, N., Imai, T., Okano, H., Yamazaki, T., and Katahira, M. (2012). Structure of Musashi1 in a complex with target RNA: the role of aromatic stacking interactions. *Nucleic Acids Res.* *40*, 3218–3231.
- Okamoto, K., Nagai, T., Miyawaki, A., and Hayashi, Y. (2004). Rapid and persistent modulation of actin dynamics regulates postsynaptic reorganization underlying bidirectional plasticity. *Nat. Neurosci.* *7*, 1104–1112.
- Pollard, T.D., and Beltzner, C.C. (2002). Structure and function of the Arp2/3 complex. *Curr. Opin. Struct. Biol.* *12*, 768–774.
- Roy, P.J., Stuart, J.M., Lund, J., and Kim, S.K. (2002). Chromosomal clustering of muscle-expressed genes in *Caenorhabditis elegans*. *Nature* *418*, 975–979.
- Sakakibara, S., Nakamura, Y., Satoh, H., and Okano, H. (2001). RNA-binding protein Musashi2: developmentally regulated expression in neural precursor cells and subpopulations of neurons in mammalian CNS. *J. Neurosci.* *21*, 8091–8107.
- Sakakibara, S., Nakamura, Y., Yoshida, T., Shibata, S., Koike, M., Takano, H., Ueda, S., Uchiyama, Y., Noda, T., and Okano, H. (2002). RNA-binding protein Musashi family: roles for CNS stem cells and a subpopulation of ependymal cells revealed by targeted disruption and antisense ablation. *Proc. Natl. Acad. Sci. USA* *99*, 15194–15199.
- Shuai, Y., Lu, B., Hu, Y., Wang, L., Sun, K., and Zhong, Y. (2010). Forgetting is regulated through Rac activity in *Drosophila*. *Cell* *140*, 579–589.
- Stetak, A., Hörndli, F., Maricq, A.V., van den Heuvel, S., and Hajnal, A. (2009). Neuron-specific regulation of associative learning and memory by MAGI-1 in *C. elegans*. *PLoS ONE* *4*, e6019.
- Vukojevic, V., Gschwind, L., Vogler, C., Demougin, P., de Quervain, D.J., Papassotiropoulos, A., and Stetak, A. (2012). A role for α -adducin (ADD-1) in nematode and human memory. *EMBO J.* *31*, 1453–1466.
- Wang, H., Hu, Y., and Tsien, J.Z. (2006). Molecular and systems mechanisms of memory consolidation and storage. *Prog. Neurobiol.* *79*, 123–135.
- Wicks, S.R., de Vries, C.J., van Luenen, H.G., and Plasterk, R.H. (2000). CHE-3, a cytosolic dynein heavy chain, is required for sensory cilia structure and function in *Caenorhabditis elegans*. *Dev. Biol.* *221*, 295–307.
- Wixted, J.T. (2004). The psychology and neuroscience of forgetting. *Annu. Rev. Psychol.* *55*, 235–269.
- Yamaguchi, H., Miki, H., Suetsugu, S., Ma, L., Kirschner, M.W., and Takenawa, T. (2000). Two tandem verprolin homology domains are necessary for a strong activation of Arp2/3 complex-induced actin polymerization and induction of microspike formation by N-WASP. *Proc. Natl. Acad. Sci. USA* *97*, 12631–12636.
- Yoda, A., Sawa, H., and Okano, H. (2000). MSI-1, a neural RNA-binding protein, is involved in male mating behaviour in *Caenorhabditis elegans*. *Genes Cells* *5*, 885–895.